

ORIGINAL ARTICLE

Effects of Bone Morphogenetic Protein-2 on Neovascularization During Large Bone Defect Regeneration

Hope B. Pearson, MS,¹ Devon E. Mason, MS,^{1,2} Christopher D. Kegelman, MS,^{2,3} Liming Zhao, PhD,⁴ James H. Dawahare, BS,¹ Melissa A. Kacena, PhD,^{4,5} and Joel D. Boerckel, PhD¹⁻³

Insufficient blood vessel supply is a primary limiting factor for regenerative approaches to large bone defect repair. Recombinant bone morphogenetic protein-2 (BMP-2) delivery induces robust bone formation and has been observed to enhance neovascularization, but whether the angiogenic effects of BMP-2 are due to direct endothelial cell stimulation or due to indirect paracrine signaling remain unclear. In this study, we evaluated the effects of BMP-2 delivery on vascularized bone regeneration and tested whether BMP-2 induces neovascularization directly or indirectly. We found that delivery of BMP-2 (5 μ g) enhanced both bone formation and neovascularization in critically sized (8 mm) rat femoral bone defects; however, BMP-2 did not directly stimulate angiogenesis *in vitro*. In contrast, conditioned medium from both mesenchymal progenitor cells and osteoblasts induced endothelial cell migration *in vitro*, suggesting a paracrine mechanism of BMP-2 action. Consistent with this inference, codelivery of BMP-2 with endothelial colony forming cells to a heterotopic site, distant from the skeletal stem cell-rich bone marrow niche, induced ossification but had no effect on neovascularization. Taken together, these data suggest that paracrine activation of osteoprogenitor cells is an important contributor to neovascularization during BMP-2-mediated bone regeneration.

Keywords: BMP-2, angiogenesis, bone defect, bone regeneration

Impact Statement

In this study, we show that bone morphogenetic protein-2 (BMP-2) robustly induces neovascularization during tissue-engineered large bone defect regeneration, and we found that BMP-2 induced angiogenesis, in part, through paracrine signaling from osteoprogenitor cells.

Introduction

CRITICAL-SIZED BONE defects that do not heal without intervention have prolonged morbidity and are extremely costly.^{1,2} Approximately 1.5 million bone grafting operations are performed annually in the United States.³ Although autologous bone is the “gold standard” for bone grafting in segmental bone loss and intervertebral fusion, this treatment is limited by insufficient supply for large defects as well as substantial donor site pain and morbidity.⁴ Allografts are, therefore, often required to bridge the defect,

but with limitations including graft rejection, disease transmission, and lower rates of healing compared with autografts due to a failure to revascularize and remodel, leading to refracture.⁵ Alternative regenerative strategies are needed, and tissue engineering has emerged as a promising alternative.

The most successful bone tissue-engineering strategy to date is biomaterial-based delivery of osteoinductive growth factors, including members of the bone morphogenetic protein (BMP) family, such as BMP-2. BMP-2 is clinically approved for lumbar spine fusion, open tibial fractures and some

¹Department of Aerospace and Mechanical Engineering, University of Notre Dame, Notre Dame, Indiana.

²Department of Bioengineering, School of Engineering and Applied Sciences, University of Pennsylvania, Philadelphia, Pennsylvania.

³Department of Orthopaedic Surgery, Perelman School of Medicine, University of Pennsylvania, Philadelphia, Pennsylvania.

⁴Department of Orthopaedic Surgery, Indiana University School of Medicine, Indianapolis, Indiana.

⁵Richard L. Roudebush VA Medical Center, Indianapolis, Indiana.

nonunions, and maxillofacial regeneration, but is often used off-label for large segmental defects and fractures in patients with comorbidities likely to produce nonunion.^{6,7} This approach, in which soluble growth factor is delivered through absorbable collagen sponge, robustly induces new bone formation through osteoprogenitor cell recruitment and local stimulation of osteogenic differentiation and matrix production.^{8,9}

New blood vessel formation and volumetric perfusion are critical for the regeneration of large bone defects as osteoblasts require <300 μm proximity to a capillary supply for survival.¹⁰ BMP-2 delivery enhances new blood vessel formation in bone defects,¹¹ but whether BMP-2 directly stimulates endothelial cell angiogenesis or indirectly through paracrine signaling from activated osteoprogenitor cells remains controversial.^{12–16}

In this study, we evaluated the effects of BMP-2 delivery on neovascularization of large bone defects and whether BMP-2 directly induces endothelial cell activation or indirectly activates paracrine signaling from osteogenic cells. In this study, we show that delivery of BMP-2 (5 μg per defect) enhanced both bone formation and neovascularization in large femoral bone defects; however, BMP-2 did not directly stimulate angiogenesis *in vitro*. In contrast, human MSC and mouse osteoblast-conditioned medium induced endothelial cell migration and tubular network formation *in vitro*, suggesting a paracrine mechanism. Finally, BMP-2 codelivery with endothelial colony forming cells (ECFCs) to a heterotopic site, distant from the bone marrow niche, induced ossification but had no effect on neovascularization. Together these data suggest that BMP-2-induced neovascularization during bone regeneration occurs secondary to mesenchymal progenitor cell activation and bone formation rather than direct endothelial cell activation.

Materials and Methods

Rat femoral segmental bone defect model

Critical-sized (8 mm) bilateral femoral defects were created in 14-week-old female SASCO Sprague Dawley rats and stabilized with custom internal fixation plates as described previously.¹⁷ In brief, fixation plates were affixed to the anterolateral surface using four bicortical screws. Mid-diaphyseal segmental defects, 8 mm in length, were created using an oscillating saw under saline irrigation. Lyophilized Type I collagen scaffolds (average pore size 61.7 μm , 93.7% pore volume; DSM Biomedical) were cut into cylinders ($h=9$ mm, $d=5$ mm) and hydrated with 100 μL of phosphate-buffered saline (PBS) containing BMP-2 or rat serum albumin carrier. BMP-2 was purchased (R&D Systems, Medtronic), reconstituted in sterile PBS, and diluted to 5 $\mu\text{g}/100$ μL . The hydrated collagen scaffolds were then placed in the femoral defect and the muscles and incision were sutured closed and secured with wound clips. Wound clips were removed 2 weeks postsurgery. For pain management, animals were given subcutaneous injections of buprenorphine (0.01–0.03 mg/kg) every 8 h for 3 days. All procedures were reviewed and approved by the Institutional Animal Care and Use Committees, which follows the National Institutes of Health guidelines on the human care and use of laboratory animals.

In vivo microCT imaging

Longitudinal microCT imaging was performed at 4 and 8 weeks postsurgery. Scanning was performed at high resolution, using voxel sizes of either 20 or 39 μm (depending on experiment), 79.9 mm FOV diameter 70 kVp 114 μA , and 8 W energy. Measurements were calibrated at 70 kVp, BH 1200 mgHA/ccm scaling with a 200 ms integration time for a slice thickness of 0.02 or 0.039 mm.

The defect region of interest was defined by the minimum distance across all samples using contours that captured all bone formed in each transverse slice. Bone formation at the proximal and distal ends of nonbridged samples was also assessed for bone volume and bone mineral density by individual contouring, beginning at the last slice containing original cortical bone and continuing to the last slice containing new bone forming the capped end.

MicroCT angiography

Contrast-enhanced microCT angiography was performed to quantify and visualize three-dimensional neovascular structures, as described previously.¹¹ In brief, the ascending aorta was catheterized through the left ventricle of the heart, and serial solutions of heparin (200 mL), 10% neutral buffered formalin (100 mL), and PBS (100 mL). The vasculature was then manually perfused with the lead chromate-containing radiodense contrast agent, Microfil MV-122 (Flowtech). The contrast agent was diluted (4:1) to attenuate X-rays at the same threshold as newly formed bone, to enable simultaneous reconstruction.^{11,18} MicroCT scans were performed to register both bone and vascular structures together using a voxel size of 15.6 or 20 μm , medium resolution, 31.9 mm FOV diameter, 70 kVp 114 μA , and 8 W energy. Measurements were calibrated at 70 kVp, BH 1200 mgHA/ccm scaling with a 200 ms integration time for a slice thickness of 0.0156 or 0.02 mm. Next, the mineralized tissues were fully decalcified using EDTA or Cal-Ex I (Fisher Scientific) with gentle agitation at room temperature for 4–8 weeks. The limbs were then rescanned to image and quantify the vasculature alone. Bone volume in each defect was then calculated by subtracting the vessels-only scan from the composite bone-and-vessel scan.

The bone volume was analyzed using 10 mm diameter contour circles to ensure inclusion of all bone formed. The vessel analysis was performed using 5 mm diameter contour circles centered in the defect.

In vivo experimental design

Three separate *in vivo* experiments were performed. The first two featured BMP-2 delivery to femoral segmental defects, and the third evaluated vascularized bone formation in a heterotopic (subcutaneous) site.

Segmental defect study 1

Bilateral segmental bone defects were created in the femora of eight rats. Each animal received a treatment condition in one limb (5 μg BMP-2) and PBS control in the contralateral limb. MicroCT angiography was performed at week 3 postsurgery. One animal was euthanized due to complications during surgery, and two animals were excluded from vascular analysis due to incomplete contrast agent

perfusion. One PBS-treated limb was also excluded from vascular analysis due to ruptured vessels during perfusion. Vessel analysis and statistics were, therefore, completed on five animals ($n=4-5$).

Segmental defect study 2

Bilateral segmental bone defects were created in the femora of 16 rats. Six animals received PBS only in both limbs to assess potential systemic effects of BMP-2 treatment. Ten animals received BMP-2 treatment condition in one limb (5 μg BMP-2) and PBS control in the contralateral limb ($n=10$ for BMP-2/PBS paired). In this study, *in vivo* microCT analysis was performed at weeks 4 and 8 post-surgery, and high-resolution microCT angiography was then performed at week 8 postsurgery. Four animals died due to complications, and three animals were excluded from microCT angiography analysis due to incomplete contrast agent perfusion. Longitudinal microCT analysis and statistics were evaluated in 12 animals (BMP-2 treated $n=9$, PBS treated $n=3$). Vessel analysis and statistics were evaluated in nine animals (BMP-2 treated $n=7$, PBS-only treated $n=2$).

Subcutaneous study

Type I collagen hydrogel matrices (2.5 mg/mL, Geni-Phys) were polymerized in 24-well plates into disk-shaped constructs of 240 μL volume. Matrices were polymerized containing four conditions: with or without ECFCs (1.6×10^6 cells/mL; 384,000 cells per construct) and with or without BMP-2 (100 ng/mL; 24 ng per construct). Collagen matrices were then cultured for 24 h before implantation in 500 μL endothelial growth medium-2 (EGM-2) containing 10% fetal bovine serum (FBS). For implantation of human ECFCs *in vivo*, Rowett Nude (RNU) rats were used to minimize immune reactions. Fourteen-week-old female RNU rats ($n=6$) received four implants per animal, with two implants placed subcutaneously over each back flank, respectively. In brief, a single incision was made on the dorsum, and two separate pockets were bluntly dissected above each flank such that each subcutaneous pocket was separated by intact fascia. The hydrogels were placed inside custom polysulfone rings to enable region of interest determination ($h=1.77$ d_i=11 mm, d_o=13 mm) and deposited into each pocket. Conditions were evenly randomized between animals. For pain management, animals were given subcutaneous injections of buprenorphine (0.01 mg/kg) every 8 h for 2 days. MicroCT angiography was performed at week 4.

ECFC isolation and culture

Primary human ECFCs, isolated from human umbilical cord blood,¹⁹ were purchased from Indiana University (Indianapolis, IN). ECFCs were cultured as previously described.^{19,20} In brief, ECFCs were seeded on type I collagen (5 $\mu\text{g}/\text{cm}^2$)-coated tissue culture polystyrene and cultured in EGM (EGM-2 with bullet kit; Lonza; CC-3162), supplemented with 1% penicillin/streptomycin (Corning) and 10% defined FBS (Thermo Fisher). ECFCs were used between passages 6 and 8.

ECFC wound migration assay

ECFC migration was evaluated in the wound migration assay, as described previously.^{18,21} In brief, passage P6-P8 ECFCs were plated in six-well plates and allowed to grow to 80% confluence. After being serum starved for 2 h in endothelial basal medium-2 (EBM-2), wounds were created in the cell monolayer by dragging a 200 μL pipette tip across the well both vertically and horizontally to form a cross. Cells were then washed with EBM-2 to remove any dead cells and supplemented with either EBM-2 only (negative control), 2% serum in EBM-2, vascular endothelial growth factor (VEGF) (100 ng/mL) in EBM-2, cysteine-rich angiogenic inducer 61 (Cyr61) (100 ng/mL) in EBM-2, or BMP-2 (100 or 200 ng/mL) in EBM-2. Cell migration was monitored by taking images at 0, 4, 8, and 12 h. Percentage wound closure was calculated by measuring the wound area at each time point and dividing by the initial wound area at the time of scratch. Wound closure rate was calculated by multiplying the percentage wound closure by the initial scratch width and dividing by the migration time. Notably, we showed previously that proliferation blockade did not alter ECFC migration in this assay.²¹

ECFC tubular network formation assay

Tubulogenesis was evaluated using the matrigel tube formation assay as described previously.^{18,21} In brief, reduced growth factor basement membrane matrix (Trevigen 3433-001-R1) was polymerized in a 96-well plate (60 μL) at 37°C for 30 min. Passage P6-P8 ECFCs were plated on the polymerized basement membrane matrix at 50,000 cells/cm² (16,190 cells/well). Treatment medium was added according to seven groups: EBM-2 only (control), 2% serum in EBM-2, or EBM-2 supplemented with VEGF (100 ng/mL), or BMP-2 (100, 200 ng/mL). Cells were incubated at 37°C and imaged at 4 and 8 h. Total vessel length, average vessel length, number of nodes, number of branches, and number of branches per node were measured using ImageJ.²²

SMAD1/5/9 immunolocalization

ECFCs were cultured for 24 h on glass coverslips with an initial seeding density of 50,000 cells/cm² and serum starved for 2 h. Cells were then treated with 10 ng/mL of BMP-2 for 0, 15, 30, 45, and 60 min. Cells were fixed with 37°C prewarmed 3.7% formaldehyde, 5% sucrose for 20 min at room temperature, permeabilized and blocked with 0.3% triton-x, and 5% goat serum for 1 h at room temperature. Cells were washed with PBS and treated with SMAD1/5/9 primary antibody at a 1:200 dilution (abcam #ab80255) at 4°C overnight and visualized using a secondary Alex Fluor 594 antibody at 10 $\mu\text{g}/\text{mL}$ for 30 min at room temperature. Cells were counterstained with fluorescein isothiocyanate-phalloidin (to visualize F-actin) and 4',6-diamidino-2-phenylindole (nuclei). SMAD intensity and localization were quantified using ImageJ.²²

Marrow stromal cell and calvarial osteoblast culture

Human bone marrow stromal cells (hMSCs, ATCC PCS-500-012) were purchased from ATCC and cultured according to manufacturer protocols, using ATCC MSC Growth Kit (ATCC PCS-500-041). In brief, hMSCs were cultured in basal medium (BM) supplemented with 7% FBS,

5 ng/mL basic fibroblast growth factor, 15 ng/mL insulin-like growth factor-1, and 2.4 mM L-alanyl-L-glutamine. Cells were used between passages 2 and 4 to generate conditioned medium as detailed hereunder.

Neonatal murine calvarial cells were isolated and cultured as described previously.^{23–25} In brief, calvariae from 2-day-old C57BL/6 mice were dissected, pretreated with EDTA, then subjected to sequential collagenase digestions (200 U/mL). Fractions 3–5 (i.e., digestions 20–35, 35–50, and 50–65 min) were collected. These freshly prepared primary cells (calvarial osteoblasts [COBs]) are >95% osteoblasts or osteoblast precursors as previously demonstrated,²³ and were used to generate conditioned medium as detailed hereunder.

Conditioned medium experiments

Wound migration and tube formation experiments were repeated using conditioned medium from hMSCs or mouse COBs. First, conditioned medium was isolated from passages 2 to 4 hMSCs (ATCC), which were seeded at 80% confluence in six-well plates for 3 or 6 days with or without 100 ng/mL of BMP-2. EBM-2 was then supplemented with 30% hMSC conditioned medium for migration and tube formation assays. Next, mouse COB-conditioned medium experiments were performed by seeding 400 K freshly isolated COB into 10 cm tissue culture dishes in α -MEM supplemented with 10% serum and penicillin–streptomycin–glutamine. Conditioned medium was collected after 6 days of culture. Next, EBM-2 was supplemented with mouse COB conditioned medium at either 10% or 30% for migration assays and at 30% for tube formation assays.

Statistical methods

Differences between groups were evaluated by paired Student's *t*-test or one way analysis of variance followed by Tukey's *post hoc* test for multiple comparisons, when assumptions for homoscedasticity and normality were met by Brown-Forsythe and D'Agostino and Pearson tests, respectively. When assumptions for normality and homoscedasticity were not met, data were log transformed and the parametric analyses were repeated. Kruskal–Wallis non-parametric and Dunn's multiple comparisons tests were used when normality and homoscedasticity conditions were not achieved by log transformation. *p*-Values <0.05 were considered significant. Significance indicator letters shared in common between groups indicate no significant difference in pairwise comparisons.

Results

The objectives of this study were first to determine the extent to which BMP-2 enhances vascularized bone regeneration and second to test whether the neovascular response to BMP-2 treatment is direct (by stimulating endothelial cell angiogenesis) or indirect (through paracrine signaling from other cells).

Effects of BMP-2 on vascularized bone regeneration at week 3

In our first experiment, we delivered BMP-2 (5 μ g) to large bone defects and evaluated bone formation and neovascularization at week 3 postsurgery. BMP-2 delivery

significantly increased bone formation compared with contralateral PBS controls (Fig. 1).

To determine whether BMP-2 enhanced blood vessel formation, we quantified the amount and morphology of the neovascular structures in the defect at week 3 by microCT angiography. BMP-2 delivery significantly increased neovascular volume fraction, vascular connectivity, and vessel number, but diameter and spacing were not significantly different (Fig. 2A–F).

Effects of BMP-2 on vascularized bone regeneration at week 8

We next evaluated the effects of BMP-2 (5 μ g) delivery on vascularized bone regeneration for 8 weeks by longitudinal *in vivo* microCT imaging and microCT angiography at week 8. BMP-2 treatment increased bone formation amount and rate compared with contralateral PBS controls (Fig. 3A). Animals with paired PBS-only scaffolds in both limbs showed bone formation similar to contralateral controls for BMP-2-treated limbs, suggesting no systemic effects of BMP-2 on bone regeneration. Postmortem bone volume for BMP-2-treated limbs was significantly greater ($p < 0.001$) than that of PBS controls (Fig. 3B). Bone mineral density was significantly lower ($p < 0.001$) for the BMP-2-treated defects, indicative of new woven bone formation (Fig. 3C). Representative images of bone formation local mineral density mapping on a sagittal cut plate at week 8 are shown (Fig. 3D).

By week 8, 5 μ g BMP-2 treatment significantly elevated vascular volume fraction, connectivity, and number (Fig. 4A–C), and reduced vessel spacing and degree of anisotropy (Fig. 4D, F). Vessel diameter was not significantly different between groups (Fig. 4E). Animals with paired PBS-only scaffolds in both limbs were not included in the quantitative analysis due to the small sample size ($n = 2$), but their values

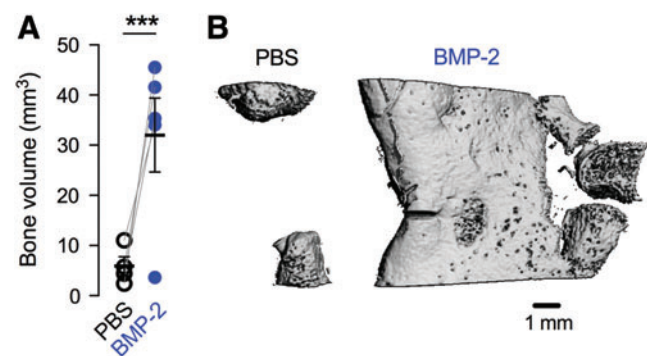


FIG. 1. Effects of 5 μ g BMP-2 delivery on bone formation at week 3. (A) MicroCT-measured bone volume. Comparisons among and between groups were performed by two-way ANOVA with matched pairs and Bonferroni's multiple comparisons test. $n = 4–5$ per group. Each replicate is shown with summary statistics represented as mean \pm SEM. ***Indicates $p \leq 0.001$ versus all other groups. (B) Representative microCT images of bone formation in the defect. ANOVA, analysis of variance; BMP-2, bone morphogenetic protein-2; SEM, standard error of the mean. Color images are available online.

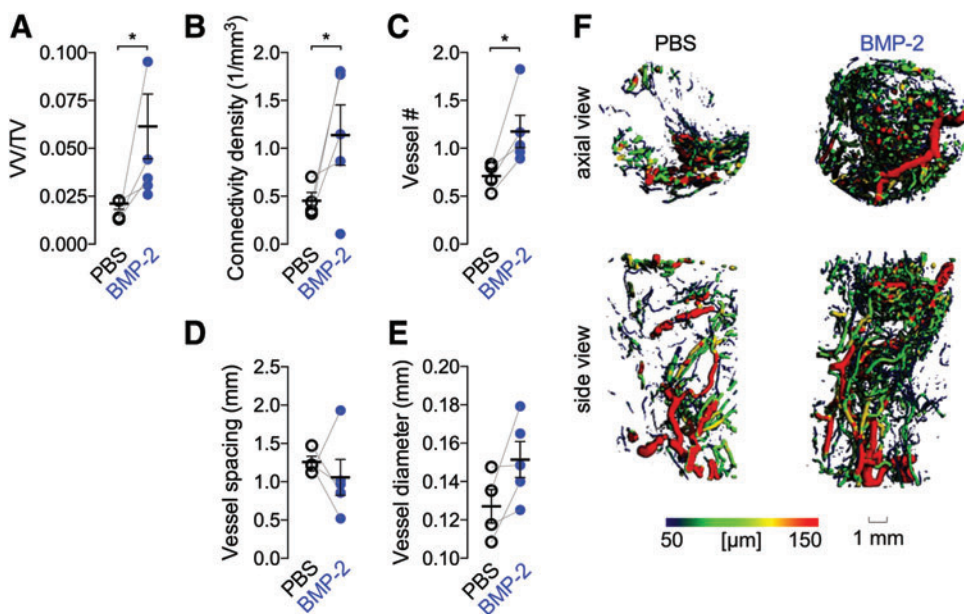


FIG. 2. Effects of 5 μ g BMP-2 delivery on blood vessel formation at week 3. (A) Vessel volume fraction (vessel volume/total volume). (B) Vascular connectivity density. (C) Vessel number. (D) Vessel spacing. (E) Vessel diameter. Each replicate is shown with summary statistics represented as mean \pm SEM. Paired limbs are connected by *gray lines* and mean and standard error of the mean are indicated in *black*. Comparisons among and between groups were performed by paired Student's *t*-tests. *n* = 4–5 per group. *Indicates $p \leq 0.05$. (F) Representative microCT images of defect vascularization with local vascular diameter mapping. Color images are available online.

were comparable with the contralateral controls of the BMP-2 animals (data not shown).

ECFC responsiveness to BMP-2

BMP-2 signals, in part, by inducing nuclear localization of the transcription factors SMAD1/5/9. To test whether BMP-2 stimulation induces canonical SMAD signaling in endothelial cells, we quantified SMAD1/5/9 nuclear localization in ECFCs by immunofluorescence after 10 ng/mL of BMP-2 stimulation for 0, 15, 30, 45, and 60 min. BMP-2 treatment significantly increased the ratio of nuclear:cytosolic SMAD1/5/9 after 60 min (Fig. 5).

Effects of BMP-2 on angiogenesis in vitro

We next tested whether BMP-2-induced signaling was effective to stimulate ECFC migration and tube formation *in vitro*. Cells were stimulated with either low (100 ng/mL) or high (200 ng/mL) doses of BMP-2 and cell migration and tube formation were quantified for 12 and 8 h, respectively, in comparison with serum-free BM negative controls and VEGF (100 ng/mL) or 2% FBS positive controls. Both positive controls significantly induced migratory wound closure, but BMP-2 treatment did not alter cell migration (Fig. 6A, B). FBS positive controls significantly increased tube length, but BMP-2 treatment did not (Fig. 6C–F).

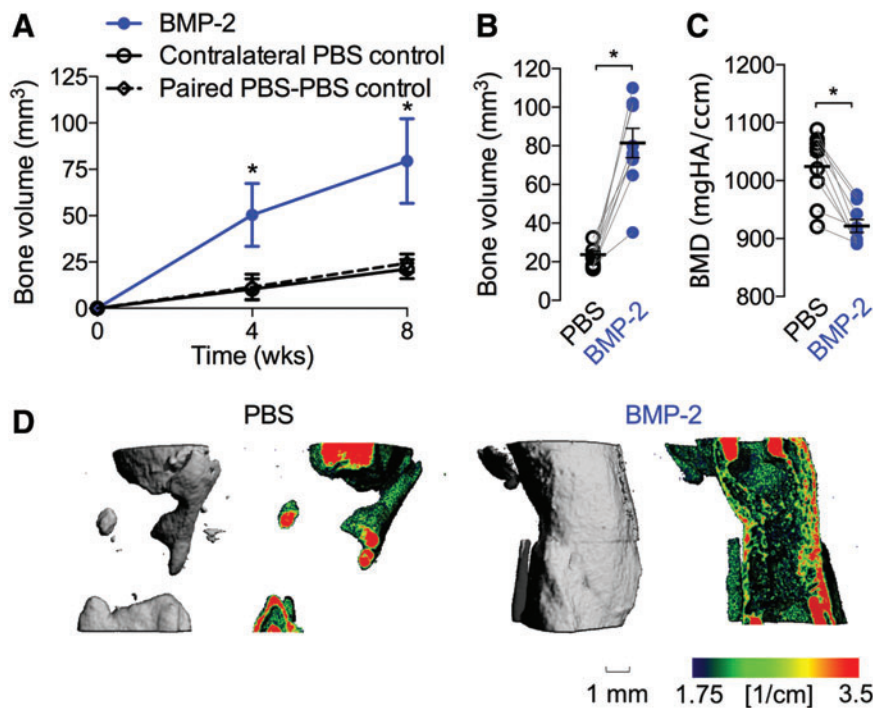
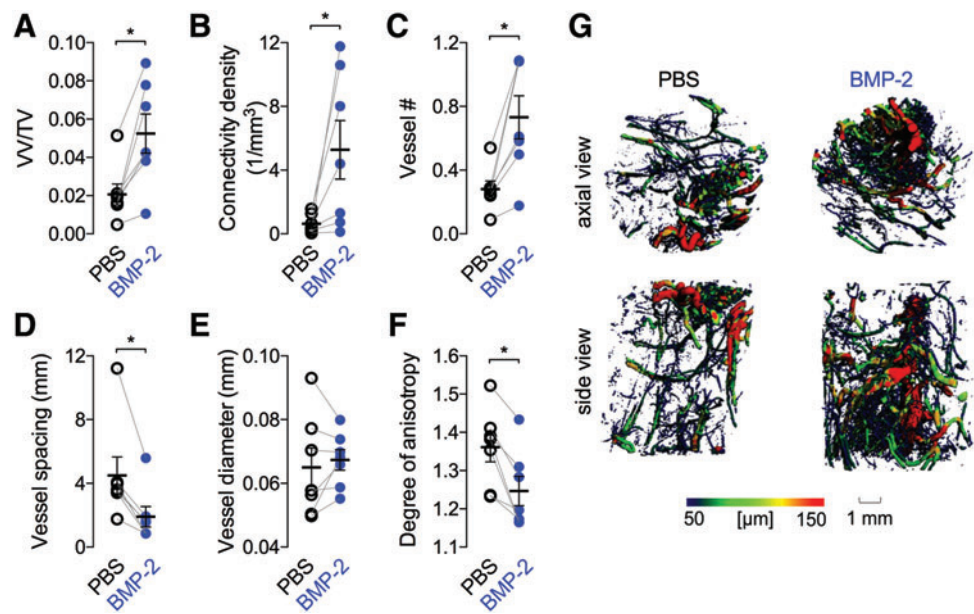


FIG. 3. Effects of 5 μ g BMP-2 delivery on bone formation at week 8. (A) Longitudinal *in vivo* microCT-measured bone volume. Summary statistics represented as mean \pm SEM. (B) Postmortem bone volume at week 8. (C) Postmortem bone mineral density at week 8. (D) Representative microCT images of bone formation and local mineral density mapping. Each replicate is shown with summary statistics represented as mean \pm SEM. Comparisons among and between groups were performed by repeated measures or two-way paired ANOVA and Bonferroni's multiple comparisons test. *n* = 9 per group, paired PBS–PBS controls, *n* = 3. *Indicates $p \leq 0.05$ versus all other groups at each time point. PBS, phosphate-buffered saline. Color images are available online.

FIG. 4. Effects of 5 μ g BMP-2 delivery on blood vessel formation at 8 weeks. (A) Vessel volume fraction, (B) connectivity density, (C) vessel number, (D) vessel diameter, (E) vessel diameter, (F) degree of anisotropy. Each replicate is shown with summary statistics represented as mean \pm SEM. Paired limbs are connected by *gray lines* and mean values are indicated by the horizontal lines. Comparisons among and between groups were performed by paired Student's *t*-tests. $n = 7$ –8 per group. (G) Representative microCT images of defect vascularization with local vascular diameter mapping. * $p < 0.05$. Color images are available online.



Effects of hMSC- and mouse COB-conditioned medium on angiogenesis

Since BMP-2 stimulation failed to induce angiogenesis in isolated endothelial cells, we next tested the alternative hypothesis that BMP-2 induces angiogenesis by paracrine signaling from activated progenitor cells and osteoblasts. To this end, we cultured hMSCs with or without BMP-2 stimulation for 3 or 6 days and collected conditioned medium, which we then mixed to 30% by volume with ECFC BM. We then treated ECFCs in the wound migration and tube formation assays with either hMSC-conditioned medium (hMSC-CM) or BMP-2-treated hMSC-CM (hMSC-CM+BMP-2) in comparison with 30% hMSC/70% ECFC BM as a control. Medium conditioned for 3 days had no effect on

ECFC migration (Fig. 7A) or tube formation (Fig. 7B–D), but medium conditioned by hMSCs for 6 days significantly increased both ECFC migration speed and tubular network length (Fig. 7A, B). Differences in the number of nodes and vessels per node were not significant (Fig. 7C, D).

To test whether conditioned medium from mouse COBs could similarly induce angiogenesis in a paracrine manner, we cultured COBs for 6 days and collected conditioned medium, which was mixed to 10% or 30% by volume with ECFC BM. Wound migration and tube formation assays were then performed as already described. Cob-conditioned medium at 30% significantly increased wound closure rate (Fig. 7E), but did not alter tubular network formation (Supplementary Fig. S1).

These data suggest that mesenchymal and osteoblast precursor cells may stimulate angiogenesis through paracrine mechanisms involving either secreted or exosome-encapsulated proteins. However, the identity of these factors is unclear. Recently, we found that osteoprogenitor cells express the matricellular growth factor, Cyr61, during bone growth and development.²⁶ Therefore, to test whether Cyr61 could stimulate ECFC migration in this context, we treated ECFCs with either PBS or Cyr61 (100 ng/mL) and evaluated wound closure. Similar to MSC-CM, Cyr61 treatment significantly enhanced wound closure rate (Fig. 7F).

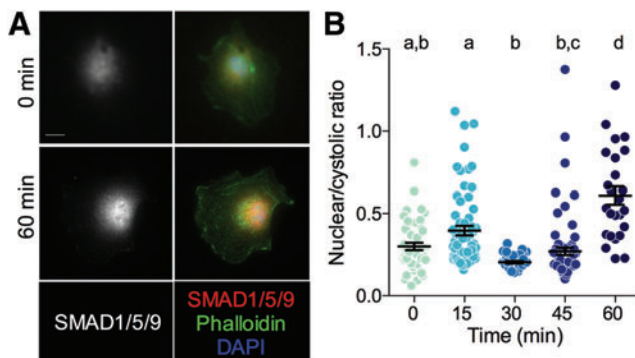


FIG. 5. BMP-2 stimulation of SMAD1/5/9 nuclear localization in ECFCs. (A) Representative images of SMAD1/5/9 staining at 0 and 60 min after BMP-2 treatment. (B) Quantification of nuclear/cytosolic ratio. Scale bar = 10 μ m. Each replicate is shown with summary statistics represented as mean \pm SEM. Significance indicator letters shared in common between groups indicate no significant difference in pairwise comparisons ($p > 0.05$) by Kruskal–Wallis and Dunn's multiple comparisons test. $n = 25$ –76. ECFCs, endothelial colony forming cells. Color images are available online.

Effects of BMP-2 and/or ECFC delivery on vascularized bone formation at heterotopic sites

Together, these data suggest that BMP-2-induced neovascularization is a consequence of paracrine signaling from osteoprogenitor cells and osteoblasts rather than direct stimulation of endothelial cell angiogenesis. BMP-2 was first identified as an osteoinductive growth factor by its ability to induce bone formation at heterotopic sites, such as within the subcutaneous space.²⁷ Similarly, the subcutaneous implant model is often used to study angiogenesis *in vivo*. For example, we recently showed that human ECFCs are capable of forming a functional human neovascular plexus

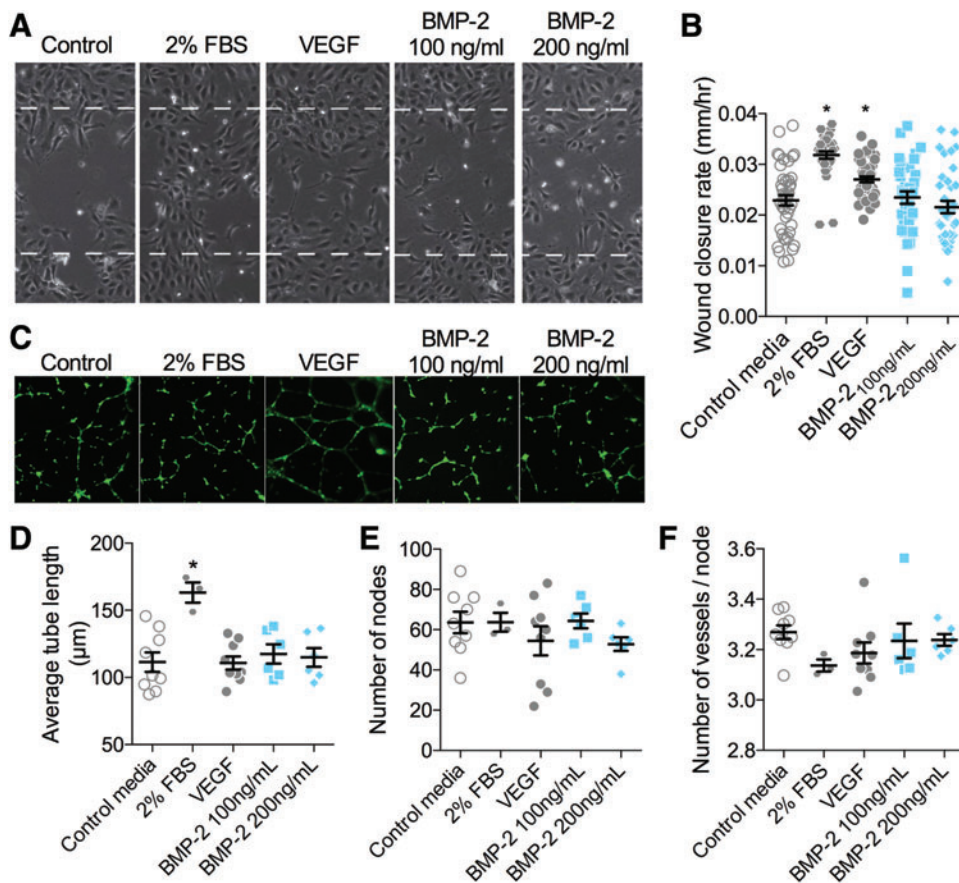


FIG. 6. Effects of BMP-2 on endothelial cell migration and tube formation. (**A**, **B**) ECFC wound closure was evaluated for 12 h (**A**) and quantified as wound closure rate (**B**). All data points are shown with mean and SEM. Initial scratch width indicated by *dashed line* ($450\ \mu\text{m}$). *Indicates $p < 0.05$ compared with negative control by Kruskal–Wallis and Dunn’s multiple comparisons test. $n = 36$ – 44 replicates, in $n = 6$ independent experiments. (**C**–**F**) ECFC tubulogenesis was evaluated for 8 h and visualized by calcein-AM staining (**C**). Network formation was quantified by average tube length (**D**), number of nodes (**E**), and number of vessels per node (**F**). Each independent replicate is shown with summary statistics represented as mean \pm SEM. Initial scratch width indicated by *dashed line* ($450\ \mu\text{m}$). *Indicates $p < 0.05$ compared with negative control by ANOVA and Tukey’s multiple comparisons test. $n = 3$ – 9 . Color images are available online.

that inosculates with the host vasculature when implanted into the subcutaneous flank of immunocompromised mice.²¹ Unlike orthotopic bone defects, in which endogenous osteoprogenitor cells and osteoblasts are relatively abundant, the subcutaneous model provides an opportunity to investigate osteogenic–angiogenic coupling in a niche that is relatively deficient in endogenous osteoprogenitor cells.

To this end, we developed collagen matrices, polymerized to fit into polysulfone disks (Fig. 8A), for subcutaneous implantation into the rear flank of RNU rats (Fig. 8B). The matrices were polymerized with or without ECFCs (384,000 cells/construct) and with or without BMP-2 (24 ng per construct) and cultured for 24 h before subcutaneous transplantation for 4 weeks ($n = 6$ per condition). Each of six animals received four implants, one from each group. At week 4, bone formation and neovascularization were evaluated by microCT angiography (Fig. 8C).

BMP-2 delivery significantly induced heterotopic bone formation, but, as expected, ECFC delivery did not (Fig. 8D). Neither BMP-2 delivery, ECFC delivery, nor their combination significantly affected neovascular volume or connectivity measured by postdecalcified microCT angiography (Fig. 8E, F).

Discussion

In this study, we evaluated the capacity of BMP-2 delivery to induce vascularized bone regeneration and tested

whether the effects were primarily direct or indirect. We found that BMP-2 induced bone formation and neovascularization in large segmental bone defects. BMP-2 failed to induce endothelial cell migration or tube formation *in vitro*, but conditioned medium from either hMSCs or mouse COB-derived cells significantly enhanced endothelial cell functions key to angiogenesis. Finally, we developed a new subcutaneous chamber model and showed that BMP-2 and/or ECFC delivery to a heterotopic site that is largely deficient in endogenous osteoprogenitor cells failed to induce neovascularization, despite BMP-2-induced osteogenesis.

Taken together, these observations identify challenges for endogenous bone tissue-engineering approaches involving growth factor delivery alone. As observed previously,^{28,29} we found that BMP-2 robustly induces bone formation in supportive environments and concomitantly enhances neovascular growth. However, in this study we conclude that BMP-2-induced angiogenesis occurs primarily through paracrine mechanisms secondary to osteoprogenitor activation rather than by direct stimulation of angiogenesis. Thus, in regenerative contexts featuring both adequate mesenchymal progenitor cell and adjacent vascular supply, BMP-2 may be sufficient to induce bone formation and physiologic neovascularization, but for injuries in which endogenous cell sources are compromised, including massive defects or multitissue polytrauma, BMP-2 delivery alone may be inadequate.

The influence of BMP-2 on angiogenesis is controversial. We and others have shown previously that BMP-2

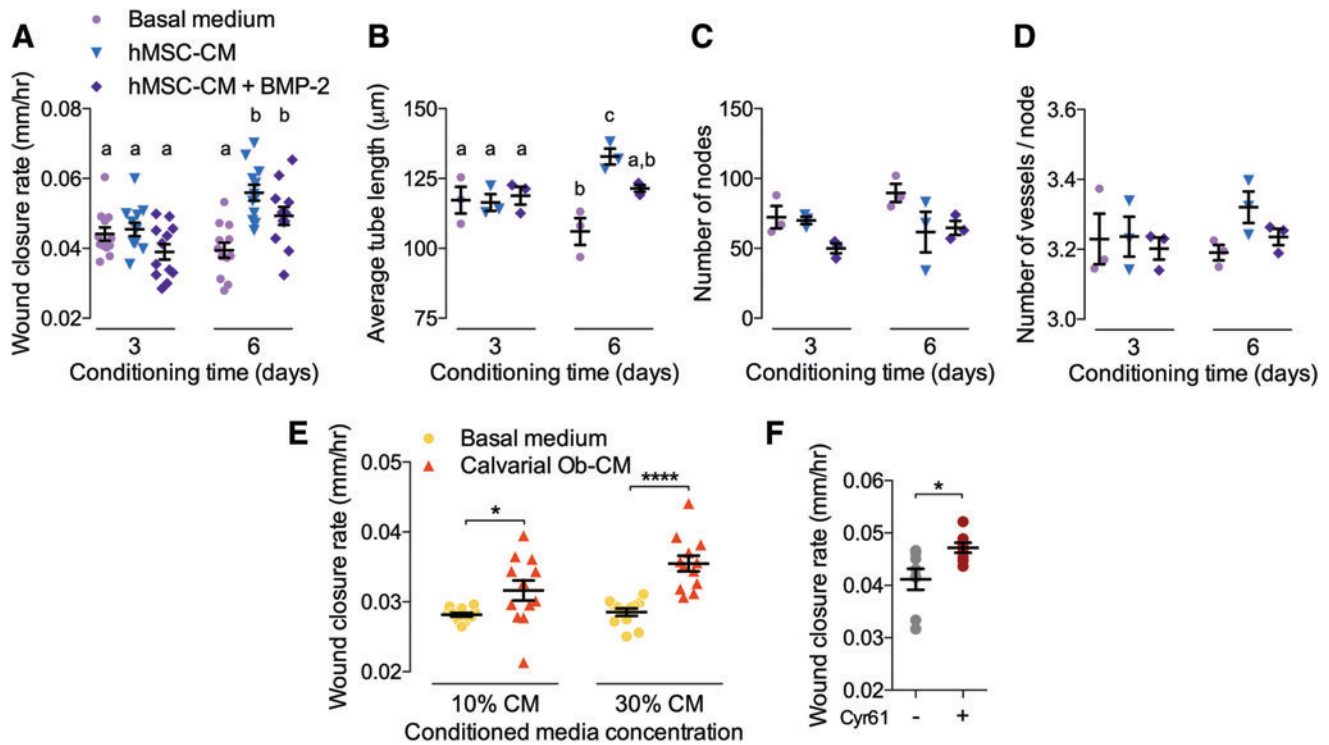
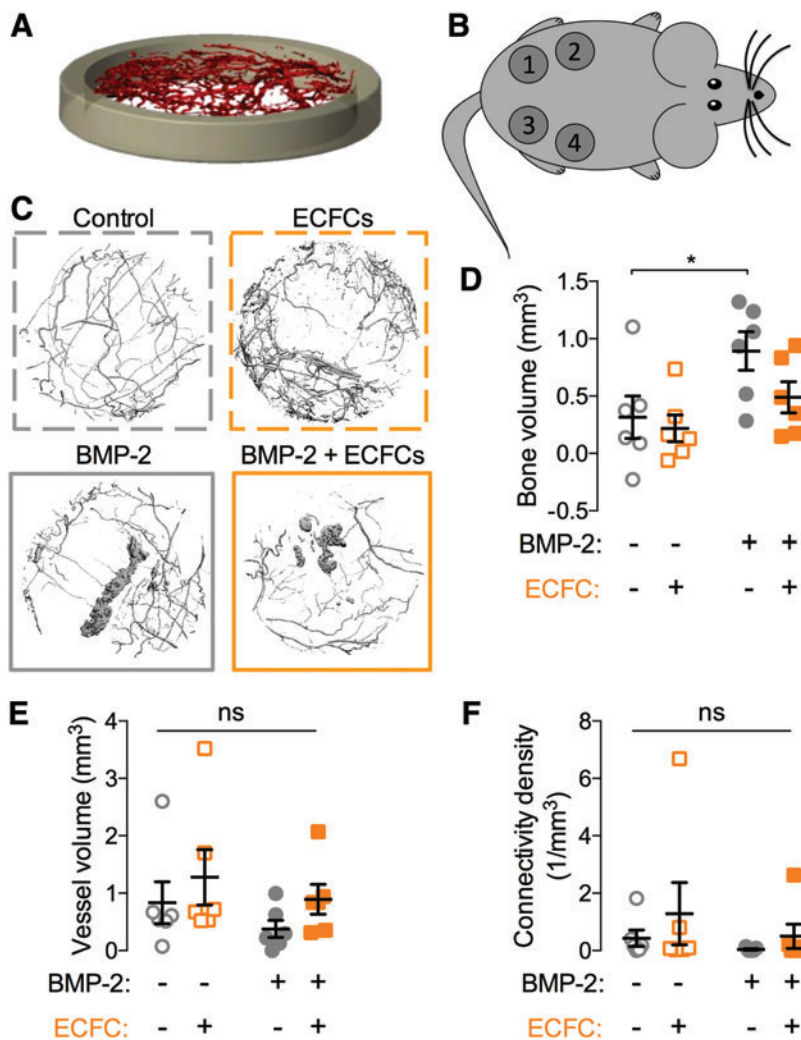


FIG. 7. Effects of hMSC- and COB-conditioned media on angiogenesis. Conditioned medium was collected from hMSCs with or without 100 ng/mL BMP-2 (hMSC-CM+BMP-2 and hMSC-CM, respectively) after 3 or 6 days culture. Migration and tube formation were evaluated using a mixture of conditioned medium (30% by volume) and ECFC basal medium (BM). (A) ECFC wound closure, quantified as wound closure rate in response to hMSC-CM with or without BMP-2 ($n = 12$ /group in $n = 4$ independent experiments). (B–D) Tubular network formation ($n = 3$ /group). (B) Average tube length. (C) Number of nodes. (D) Number of vessels per node. Similarly, conditioned medium was collected from mouse COBs after 6 days culture. Migration and tube formation were evaluated using a mixture of conditioned medium (10% or 30% by volume) and ECFC BM. (E) ECFC migration, quantified as wound closure rate, in response to COB-conditioned medium ($n = 12$ /group in $n = 4$ independent experiments). (F) ECFC migration, quantified as wound closure rate ($n = 4$ /group in $n = 2$ independent experiments) in response to treatment with recombinant human Cyr61 (100 ng/mL). Each replicate is shown with summary statistics represented as mean \pm SEM. Significance indicator letters shared in common between groups indicate no significant difference by one-way ANOVA and Tukey's multiple comparisons test. * $p < 0.05$, **** $p < 0.0001$. COB, calvarial osteoblast; Cyr61, cysteine-rich angiogenic inducer 61; hMSC-CM, human bone marrow stromal cell-conditioned medium. Color images are available online.

delivery to rat segmental bone defects can significantly enhance neovascular network formation.^{11,30} However, other studies observed no effects of BMP-2 delivery on bone defect vascularization.^{31,32} In this study, we tested the effects of BMP-2 on neovascularization in large bone defects *in vivo*, on isolated endothelial cells *in vitro*, and on ectopic angiogenesis in a niche poor in osteoprogenitor cell supply. Together, our results suggest that the primary role of BMP-2 in neovascularization during bone repair is through progenitor cell and osteoblast activation, which then stimulates angiogenesis in turn through paracrine signaling.

Studies on the direct effects of BMP-2 in endothelial cells are highly contradictory. Some report a protubulogenesis response without enhancing motility,¹⁶ whereas others observed a stimulatory effect on migration and tube formation in human microvascular endothelial cells³³ and human umbilical vein endothelial cells (HUVECs).¹³ BMP-2 has not been shown to effect HUVEC proliferation¹³ and only marginally increased DNA synthesis of human aortic endothelial cells (HAEC) and HUVECs.¹⁶ These results suggest that BMP-2 can serve as a chemoattractant and proangiogenic

cytokine, but is not uniformly a mitogenic activator for these endothelial cell types. For example, different endothelial cell types have been shown to exhibit varying responses to the same BMP ligands, potentially due to differential expression of coreceptors that mediate BMP internalization.³⁴ We did not detect effects of BMP-2 on ECFC migration or tubulogenesis, despite their responsiveness to BMP-2 at the level of signaling. Endothelial cells have BMP-2 receptors IA, IB, and II as well as the endothelial-specific TGF β type III receptor (endoglin), which facilitates the binding of BMP-2 to its receptor.³⁵ Our data confirm that BMP-2 signals through SMADs in ECFCs, but did not induce a detectable angiogenic effect in ECFCs using these assays. In contrast, conditioned medium from either hMSCs or mouse COBs enhanced ECFC migration. Conditioned medium from BMP-2-treated mesenchymal cells moderately, but not significantly, reduced measures of angiogenesis. As the data were not statistically significant, this effect could be incidental or could be associated with a shift from proliferation to differentiation status that could have reduced number of cells compared with non-differentiated MSCs in growth medium.



ECFCs are circulating endothelial cells that exhibit vasculogenic capabilities and home to sites of injury,^{19,36} motivating our use of this cell type in this study. Compared to mature, quiescent vessel cell types (typically modeled using HAECs or HUVECs), ECFCs home from the bone marrow and incorporate into sites of vascular regeneration *in vivo*.^{37,38} These cells are also capable of forming blood vessels *de novo*.^{21,39} These observations motivated our selection of these cells as an *in vitro* model system to study wound-induced neovascularization.

In addition, these cells have shown promise as a potential clinical therapeutic with their ability to incorporate into neovessels of regenerating tissues.³⁹ ECFCs have been shown to provide paracrine support to mesenchymal stem cells before establishment of neovascularization⁴⁰ and have been used in tissue-engineered scaffolds to create preformed vascular networks that have the ability to interconnect with the host vasculature *in vivo*.⁴¹ Furthermore, coordinated spatial and temporal release of BMP-2 and VEGF enhanced osteogenesis and vasculogenesis of hMSCs and ECFCs within a patterned hydrogel implant, with the greatest response seen with VEGF released for 10 days and BMP-2 released for 21 days.⁴² This further supports the importance of the time at which angiogenic and osteogenic factors are

presented. Our studies suggest that the angiogenic effects observed for ECFCs may not be primarily influenced by the presence of BMP-2.

Our data, including the paracrine signaling responses observed in MSC- and calvarial cell-conditioned medium experiments, are consistent with recent studies showing that physiologic BMP-2 induces osteoblast expression of VEGF, and subsequent angiogenesis.¹⁴ Further vascular smooth muscle and endothelial cells have been shown to express BMP-2 during bone healing,⁴³ forming a positive feedback interaction during fracture repair.⁴⁴

Ectopic bone formation and angiogenesis

In this study, we used an extraosseous implantation site (subcutaneous chamber) to minimize the effects on neovascularization of the progenitor and osteoblast cells present in the defect model. Although BMP-2 induced bone formation, we observed no detectable effect on endogenous or coimplanted endothelial cells, suggesting that neovascularization, independent of robust osteoprogenitor cell activation, was not significantly affected by the presence of BMP-2. Interestingly, the ability of rhBMP-2 to form bone in ectopic sites is inhibited by administration of TNP-470,

an antiangiogenic agent that inhibits neovascularization.⁴⁵ It is known that angiogenesis is critical for endochondral bone development⁴⁶; however, angiogenesis blockade, initiated after cell recruitment and chondrogenesis but before osteogenesis, remained permissive of ectopic bone.⁴⁵ Together, these data support the hypothesis that although angiogenesis is critical during early phases of endochondral bone healing, angiogenesis serves to recruit and support of BMP receptor positive cells that would then be able to respond to locally delivered BMP-2.⁴⁵

Limitations

In these experiments, we evaluated neovascularization by microCT angiography, which is limited by voxel resolution (here, 15 μm). By threshold selection and partial volume effects, we are likely able to detect vessels with diameters approaching this size, but this method is not able to resolve important microvessels, which may respond distinctly to BMP-2 treatment compared with vessels of larger size. We selected ECFCs as an endothelial cell model to mimic the cell types active during natural tissue regeneration. Other endothelial cell types, such as HMVEC or HUVEC, may exhibit differential angiogenic responsiveness to BMP-2 treatment. Although we have observed definitive evidence of transplanted ECFC inosculation into the mouse vasculature by lectin perfusion and immunostaining,²¹ microCT angiography may not have the resolution to resolve these neovessels. We selected a known healing dose of BMP-2 for the segmental defect studies⁴⁷; however, the precise concentrations of BMP-2 experienced by invading neovessels during bone regeneration mediated by BMP-2 delivery are unclear,^{48,49} and different BMP-2 concentrations may have direct angiogenic effects. As the purpose of the functional assays (migration and tube formation) was to ask whether the supraphysiologic doses of BMP-2 presented in the bone defect could influence endothelial cell function, we chose high doses of BMP for *in vitro* treatment (100–200 ng/mL).^{50,51} To test whether ECFCs themselves were responsive to BMP at the signaling level, we chose to present physiologic-level doses informed by the endogenous concentrations of BMP-2 measured during fracture repair.^{48,49} SMAD localization data at low BMP-2 dose indicate both that the presented BMP-2 was biologically active and that ECFCs were responsive. However, even at higher doses, this response did not induce an angiogenic effect.

Although these data suggest that BMP-2 can induce angiogenesis indirectly through paracrine signals from mesenchymal and/or osteoblast cells, the detailed mechanisms, potentially mediated by secreted and/or exosome-encapsulated proteins, remain unclear. Further work beyond the scope of this article will be required to define the responsible paracrine signals and their mechanisms of transport. We identified Cyr61 as a osteoprogenitor-secreted angiogenic agent,²⁶ and found here that Cyr61 treatment induced ECFC migration, but whether this protein is causally involved in osteoblast–endothelial cell cross-talk during bone regeneration remains unclear.

Conclusions

Taken together, this study implicates paracrine signaling as an important mechanism by which BMP-2 induces neo-

vascularization during bone repair, and identifies endogenous neovascular and mesenchymal progenitor cell supply as important contextual considerations for the efficacy of BMP-2 delivery for bone regeneration.

Acknowledgments

We thank Dr. Mervin Yoder (Indiana University) for providing ECFCs and Joseph Collins (University of Pennsylvania) for assistance with animal studies. This project was supported, in part, by American Heart Association grant 16SDG31230034 (to J.D.B.), National Institutes of Health National Center for Advancing Translational Sciences grant UL1TR001108 (to J.D.B. and M.A.K.), and by National Institutes of Arthritis, Musculoskeletal, and Skin Diseases grant R01AR074948 (to J.D.B.). This material is also the result of work supported with resources and the use of facilities at the Richard L. Roudebush VA Medical Center, Indianapolis, IN: VA Merit #BX003751 (M.A.K.).

Disclosure Statement

No competing financial interests exist.

Supplementary Material

Supplementary Figure S1

References

- Desai, B. Osteobiologics. *Am J Orthop (Belle Mead NJ)* **36**, 8, 2007.
- Kannan, R.Y., Salacinski, H.J., Sales, K., Butler, P., and Seifalian, A.M. The roles of tissue engineering and vascularisation in the development of micro-vascular networks: a review. *Biomaterials* **26**, 1857, 2005.
- USBJI. United States Bone and Joint Initiative: The Burden of Musculoskeletal Diseases in the United States (BMUS). United States Bone and Joint Initiative, 2014.
- Ehrler, D., and Vaccaro, A. The use of allograft bone in lumbar spine surgery. *Clin Orthop Relat Res* **371**, 38, 2000.
- Flierl, M.A., Smith, W.R., Mauffrey, C., *et al.* Outcomes and complication rates of different bone grafting modalities in long bone fracture nonunions: a retrospective cohort study in 182 patients. *J Orthop Surg Res* **8**, 33, 2013.
- Garrison, K.R., Donell, S., Ryder, J., *et al.* Clinical effectiveness and cost-effectiveness of bone morphogenetic proteins in the non-healing of fractures and spinal fusion: a systematic review. *Health Technol Assess* **11**, 1, iii, 2007.
- Dahabreh, Z., Calori, G.M., Kanakaris, N.K., Nikolaou, V.S., and Giannoudis, P.V. A cost analysis of treatment of tibial fracture nonunion by bone grafting or bone morphogenetic protein-7. *Int Orthop* **33**, 1407, 2009.
- Kanakaris, N.K., Paliobeis, C., Nlanidakis, N., and Giannoudis, P.V. Biological enhancement of tibial diaphyseal aseptic non-unions: the efficacy of autologous bone grafting, BMPs and reaming by-products. *Injury* **38S**, S65, 2007.
- Sen, M.K., and Miclau, T. Autologous iliac crest bone graft: should it still be the gold standard for treating non-unions? *Injury* **38**, 2, 2007.
- Phelps, E.A., and García, A.J. Engineering more than a cell: vascularization strategies in tissue engineering. *Curr Opin Biotechnol* **21**, 704, 2010.
- Boerckel, J.D., Uhrig, B.A., Willett, N.J., Huebsch, N., and Goldberg, R.E. Mechanical regulation of vascular growth

- and tissue regeneration in vivo. *Proc Natl Acad Sci U S A* **108**, E674, 2011.
12. Raida, M., Heymann, A.C., Günther, C., and Niederwieser, D. Role of bone morphogenetic protein 2 in the crosstalk between endothelial progenitor cells and mesenchymal stem cells. *Int J Mol Med* **18**, 735, 2006.
 13. Finkenzeller, G., Hager, S., and Stark, G.B. Effects of bone morphogenetic protein 2 on human umbilical vein endothelial cells. *Microvasc Res* **84**, 81, 2012.
 14. Deckers, M.M., van Bezooijen, R.L., van der Horst, G., *et al.* Bone morphogenetic proteins stimulate angiogenesis through osteoblast-derived vascular endothelial growth factor A. *Endocrinology* **143**, 1545, 2002.
 15. de Jesus Perez, V.A., Alastalo, J.C., Wu, J.D., *et al.* Bone morphogenetic protein 2 induces pulmonary angiogenesis via Wnt-beta-catenin and Wnt-RhoA-Rac1 pathways. *J Cell Biol* **184**, 83, 2009.
 16. Langenfeld, E.M., and Langenfeld, J. Bone morphogenetic protein-2 stimulates angiogenesis in developing tumors. *Mol Cancer Res* **2**, 141, 2004.
 17. Boerckel, J.D., Dupont, K.M., Kolambkar, Y.M., Lin, A.S.P., and Guldberg, R.E. In vivo model for evaluating the effects of mechanical stimulation on tissue-engineered bone repair. *J Biomech Eng* **131**, 084502, 2009.
 18. Boerckel, J.D., Chandrasekharan, U.M., Waitkus, M.S., *et al.* Mitogen-activated protein kinase phosphatase-1 promotes neovascularization and angiogenic gene expression. *Arterioscler Thromb Vasc Biol* **34**, 1020, 2014.
 19. Ingram, D.A., Mead, L.E., Tanaka, H., *et al.* Identification of a novel hierarchy of endothelial progenitor cells using human peripheral and umbilical cord blood. *Blood* **104**, 2752, 2004.
 20. Ingram, D.A., Mead, L.E., Moore, D.B., *et al.* Vessel wall-derived endothelial cells rapidly proliferate because they contain a complete hierarchy of endothelial progenitor cells. *Blood* **105**, 2783, 2005.
 21. Mason, D.E., Collins, J.M., Dawahare, J.H., *et al.* YAP and TAZ limit cytoskeletal and focal adhesion maturation to enable persistent cell motility. *J Cell Biol* **218**, 1369, 2019.
 22. Schindelin, J., Arganda-Carreras, I., Frise, E., *et al.* Fiji: an open-source platform for biological-image analysis. *Nat Methods* **9**, 676, 2012.
 23. Chitteti, B.R., Shivdasani, R.A., Wilson, K., *et al.* Osteoblast lineage cells expressing high levels of Runx2 enhance hematopoietic progenitor cell proliferation and function. *J Cell Biochem* **111**, 284, 2010.
 24. Kacena, M.A., Cheng, Y.-H., Streicher, D.A., *et al.* Megakaryocyte-osteoblast interaction revealed in mice deficient in transcription factors GATA-1 and NF-E2. *J Bone Miner Res* **19**, 652, 2004.
 25. Chitteti, B.R., Kacena, M.A., Voytik-Harbin, S.L., and Srour, E.F. Modulation of hematopoietic progenitor cell fate in vitro by varying collagen oligomer matrix stiffness in the presence or absence of osteoblasts. *J Immunol Methods* **425**, 108, 2015.
 26. Kegelman, C.D., Mason, D.E., Dawahare, J.H., *et al.* Skeletal cell YAP and TAZ combinatorially promote bone development. *FASEB J* **32**, 2706, 2018.
 27. Riley, E.H., Lane, J.M., Urist, M.R., Lyons, K.M., and Lieberman, J.R. Bone morphogenetic protein-2. *Clin Orthop Relat Res* **324**, 39, 1996.
 28. Sampath, T.K., Maliakal, J.C., Hauschka, P.V., *et al.* Recombinant human osteogenic protein-1 (hOP-1) induces new bone formation in vivo with a specific activity comparable with natural bovine osteogenic protein and stimulates osteoblast proliferation and differentiation in vitro. *J Biol Chem* **267**, 20352, 1992.
 29. Wozney, J.M. Overview of bone morphogenetic proteins. *Spine (Phila Pa 1976)* **27**, S2, 2002.
 30. Cao, L., Wang, J., Hou, J., Xing, W. and Liu, C. Vascularization and bone regeneration in a critical sized defect using 2-N,6-O-sulfated chitosan nanoparticles incorporating BMP-2. *Biomaterials* **35**, 684, 2014.
 31. Stewart, R.L., Goldstein, J., Eberhardt, A., Chu, T.-M.G., and Gilbert, S. Increasing vascularity to improve healing of segmental defect of the rat femur. *J Orthop Trauma* **25**, 472, 2011.
 32. Kempen, D.H.R., Lu, L., Heijink, A., *et al.* Effect of local sequential VEGF and BMP-2 delivery on ectopic and orthotopic bone regeneration. *Biomaterials* **30**, 2816, 2009.
 33. Rothhammer, T., Bataille, F., Spruss, T., Eissner, G., and Bosserhoff, A.-K. Functional implication of BMP4 expression on angiogenesis in malignant melanoma. *Oncogene* **26**, 4158, 2007.
 34. Dyer, L.A., Pi, X., and Patterson, C. The role of BMPs in endothelial cell function and dysfunction. *Trends Endocrinol Metab* **25**, 472, 2014.
 35. Glienke, J., Schmitt, O., Pilarsky, C., *et al.* Differential gene expression by endothelial cells in distinct angiogenic states. *Eur J Biochem* **267**, 2820, 2000.
 36. Lin, Y., Weisdorf, D.J., Solovey, A., and Hebbel, R.P. Origins of circulating endothelial cells and endothelial outgrowth from blood. [Miscellaneous Article] *J Clin Invest* **105**, 71, 2000.
 37. Asahara, T., Masuda, H., Takahashi, T., *et al.* Bone marrow origin of endothelial progenitor cells responsible for postnatal vasculogenesis in physiological and pathological neovascularization. *Circ Res* **85**, 221, 1999.
 38. Patel, C.V. Endothelial cells express a novel, tumor necrosis factor-alpha-regulated variant of HOXA9. *J Biol Chem* **274**, 1415, 1999.
 39. Yoder, M.C., Mead, L.E., Prater, D., *et al.* Plenary paper redefining endothelial progenitor cells via clonal analysis and hematopoietic stem/progenitor cell principals. *Blood* **109**, 1801, 2007.
 40. Lin, R.-Z., Moreno-Luna, R., Li, D., *et al.* Human endothelial colony-forming cells serve as trophic mediators for mesenchymal stem cell engraftment via paracrine signaling. *Proc Natl Acad Sci* **111**, 10137, 2014.
 41. Melero-Martin, J.M., De Obaldia, M.E., Kang, S.-Y., *et al.* Engineering robust and functional vascular networks in vivo with human adult and cord blood-derived progenitor cells. *Circ Res* **103**, 194, 2008.
 42. Barati, D., Shariati, S.R.P., Moeinzadeh, J., *et al.* Spatio-temporal release of BMP-2 and VEGF enhances osteogenic and vasculogenic differentiation of human mesenchymal stem cells and endothelial colony-forming cells co-encapsulated in a patterned hydrogel. *J Control Release* **223**, 126, 2016.
 43. Matsubara, H., Hogan, D.E., Morgan, E.F., *et al.* Vascular tissues are a primary source of BMP2 expression during bone formation induced by distraction osteogenesis. *Bone* **51**, 168, 2012.
 44. Beamer, B., Hettrich, C., and Lane, J. Vascular endothelial growth factor: an essential component of angiogenesis and fracture healing. *HSS J* **6**, 85, 2010.
 45. Mori, S., Yoshikawa, H., Hashimoto, J., *et al.* Anti-angiogenic agent (TNP-470) inhibition of ectopic bone

- formation induced by bone morphogenetic protein-2. *Bone* **22**, 99, 1998.
46. Bragdon, B., Lam, S., Aly, S., *et al.* Earliest phases of chondrogenesis are dependent upon angiogenesis during ectopic bone formation in mice. *Bone* **101**, 49, 2017.
 47. Boerckel, J.D., Kolambkar, Y.M., Dupont, K.M., *et al.* Effects of protein dose and delivery system on BMP-mediated bone regeneration. *Biomaterials* **32**, 5241, 2011.
 48. Santos, M.I., and Reis, R.L. Vascularization in bone tissue engineering: physiology, current strategies, major hurdles and future challenges. *Macromol Biosci* **10**, 12, 2010.
 49. Santo, V.E., Gomes, M.E., Mano, J.F., and Reis, R.L. Controlled release strategies for bone, cartilage, and osteochondral engineering—part II: challenges on the evolution from single to multiple bioactive factor delivery. *Tissue Eng Part B Rev* **19**, 327, 2013.
 50. Cheng, H., Jiang, W., Phillips, F.M., *et al.* Osteogenic activity of the fourteen types of human bone morphogenetic proteins (BMPs). *J Bone Joint Surg Am* **85**-A, 1544, 2003.
 51. Lee, K.-S., Kim, H.-J., Li, Q.-L., *et al.* Runx2 is a common target of transforming growth factor beta 1 and bone morphogenetic protein 2, and cooperation between Runx2 and Smad5 induces osteoblast-specific gene expression in the pluripotent mesenchymal precursor cell line C2C12. *Mol Cell Biol* **20**, 8783, 2000.

Address correspondence to:

Joel D. Boerckel, PhD

University of Pennsylvania

376A Stemmler Hall

36th Street and Hamilton Walk Philadelphia

Philadelphia, PA 19104

E-mail: boerckel@penmedicine.upenn.edu

Received: November 18, 2018

Accepted: March 26, 2019

Online Publication Date: June 14, 2019